

Shell-model half-lives for r-process $N = 82$ nuclei

J. J. Cuenca-García¹, G. Martínez-Pinedo¹, K. Langanke^{1,2}, F. Nowacki³, and I. N. Borzov¹

¹ Gesellschaft für Schwerionenforschung Darmstadt, Planckstr. 1, D-64259 Darmstadt, Germany

² Institut für Kernphysik, Technische Universität Darmstadt, Schlossgartenstr. 9, D-64289 Darmstadt, Germany

³ Institut de Recherches Subatomiques, IN2P3-CNRS/Université Louis Pasteur, F-67037 Strasbourg, France

Received: October 31, 2018/ Revised version: October 31, 2018

Abstract. We have performed shell-model calculations of the half-lives and neutron-branching probabilities of the r-process waiting point nuclei at the magic neutron number $N = 82$. These new calculations use a larger model space than previous shell model studies and an improved residual interaction which is adjusted to recent spectroscopic data around $A = 130$. Our shell-model results give a good account of all experimentally known half-lives and Q_β -values for the $N = 82$ r-process waiting point nuclei. Our half-life predictions for the $N = 82$ nuclei with $Z = 42$ – 46 agree well with recent estimates based in the energy-density functional method.

PACS. 21.60.Cs Shell model – 27.60.+j $90 \leq A \leq 149$ – 23.40.–s Beta decay; double beta decay; electron and muon capture

1 Introduction

The astrophysical r-process produces about half of the heavy elements in the Universe by a sequence of fast neutron-capture reactions interrupted by photodissociations and followed by β decays, running through extremely neutron-rich nuclei far off the valley of stability [1, 2]. The β decays of the r-process waiting points, associated with nuclei with magic neutron numbers $N = 50, 82$ and 126 play a crucial role for the r-process dynamics and elemental abundance distributions [3]. Despite their importance only a few half-lives of waiting points with magic neutron numbers $N = 50$ and 82 are known experimentally [4, 5], while no experimental data exist yet for the $N = 126$ waiting points. This paper is concerned with the $N = 82$ waiting points, and fortunately here the half-lives of ^{131}In , ^{130}Cd and ^{129}Ag have been measured and serve as stringent constraints for models which have to be used to predict the unknown half-lives of the other waiting points and r-process nuclei.

Beta-decays are notoriously difficult to model as they are determined by the weak low-energy tails of the Gamow-Teller strength distribution, mediated by the operator $\sigma\tau$. There have been several previous estimates for the half-lives of the $N = 82$ waiting points based on the Quasi-particle Random Phase Approximation on top of semi-empirical global models [6, 7], the energy-density functional (DF3) method [8] or the Hartree-Fock-Bogoliubov (HFB) method [9]. A comparison to the data show that the predicted half-lives are in the right order of magnitude, but are often somewhat too long. This might imply that the models underestimate the correlations among nucleons which improved study.

pull down the Gamow-Teller (GT) strength to low excitation energies. It is well known that the interacting shell model is the method of choice to describe the Gamow-Teller distribution in nuclei [10, 11, 12] and in fact, the best agreement with the measured half-lives has been achieved within a shell model approach [13].

This shell model calculation as well as the other theoretical approaches have been challenged recently by the experimental determination of the excitation energy of the first 1^+ state in ^{130}In , which carries most of the GT-strength of the ^{130}Cd decay [14]. Here, gamma rays observed in the beta decay of ^{130}Cd [14] yield an excitation energy of $E_x = 2.16$ MeV, in contrast to the shell model predictions which place this state at noticeably lower energy, $E_x = 1.4$ MeV [14] and 1.5 MeV [13]. As the half-life has a strong energy dependence which approximately scales like $(Q_\beta - E_x)^5$, where $Q_\beta = M_i - M_f$ is the difference of the masses of the parent and daughter nuclei, respectively, the misplacement of the 1^+ excitation energy has been fortuitously cancelled in the shell model calculation [13] by the use of too small a Q_β value which was taken from the Duflo-Zuker mass model yielding 7.56 MeV [15], while the experimental Q_β value is 8.34 MeV. Thus the shell model calculation of [13] despite its successful description of the half-lives of the $N = 82$ waiting point nuclei, has to be improved to account also for the recent experimental structure data concerning the respective decays. It is the aim of this manuscript to present such an

2 Formalism

We have performed large-scale shell model calculations using the code ANTOINE [16]. We have improved the previous shell model study of the half-lives of the $N = 82$ r-process nuclei [13] in several ways. At first, we used a larger model space which includes the $0g_{7/2}, 1d_{3/2,5/2}, 2s_{1/2}, 0h_{11/2}$ orbitals outside the $N = 40$ core for neutrons, thus assuming a closed $N = 82$ shell configuration in the parent nucleus. For protons our model space was spanned by the $0g_{9/2,7/2}, 1d_{3/2,5/2}, 2s_{1/2}$ orbitals. Thus our model space avoids spurious center-of-mass excitations by omitting the $h_{11/2}$ orbit for protons and the $g_{9/2}$ orbit for neutrons. Secondly, we have performed the calculations of the parent ground states and the GT strength distributions in the daughter nucleus for the $N = 82$ parents with charge numbers $Z = 43 - 49$ including all possible correlations within the defined model space, a clear improvement with respect to the calculations in ref. [13]. But most importantly we have modified the residual interaction adopted in our studies to reproduce relevant experimental nuclear structure information. These modifications were guided by the observation that for the nuclei of interest here, the halfives are dominated by Gamow-Teller transitions to states at low excitation energy in the daughter nuclei and that these transitions are mainly determined by a single transition matrix element in which a $g_{7/2}$ neutron is changed into a $g_{9/2}$ proton. This implies that the transition matrix elements are quite insensitive to the relative position of the $g_{7/2}$ neutron orbit but its position determines the excitation energy of the daughter states and the Q_β value for the evaluation of the half-lives. Starting from the interaction used in the previous shell-model calculations [13] we have implemented several monopole modifications aiming to reproduce the known Q_β values of ^{131}In [17] and ^{130}Cd [14], the position of the $h_{11/2}$ neutron orbit [17] and the experimental excitation energy of the first 1^+ state in ^{130}In (for details see ref. [18]). This has resulted in two effective interactions: one that allows proton excitations from the $p_{1/2}$ orbit (that means uses a ^{88}Sr core) and another one where these excitations are suppressed (uses a ^{90}Zr core). Fig. 1 compares our calculated low-energy spectrum of ^{130}In with the data and find good agreement for the excitation energies of the first 3^+ state. Importantly our improved shell model calculations also reproduces the unexpectedly high excitation energy of the first 1^+ state, which is of key importance for the calculation of the ^{130}Cd half-life. However, the low energy 5^+ state and the states with possible assignments 0^- and 1^- are missed by the calculation that uses a ^{90}Zr core. These are reproduced by the interactions that includes the $p_{1/2}$ orbital which is energetically relatively close to the $g_{9/2}$ orbital, but carries the opposite parity. Once, the $p_{1/2}$ orbital is included in the model space we are forced to truncate the number of protons excited across the $g_{9/2}$ shell gap. The calculations shown at the right of figure 1 where performed allowing for 6 protons to be excited from the $p_{1/2}$ and $g_{9/2}$ orbitals. Shell model calculations performed within the same model space and using the same interaction also reproduce the recently measured spectrum of

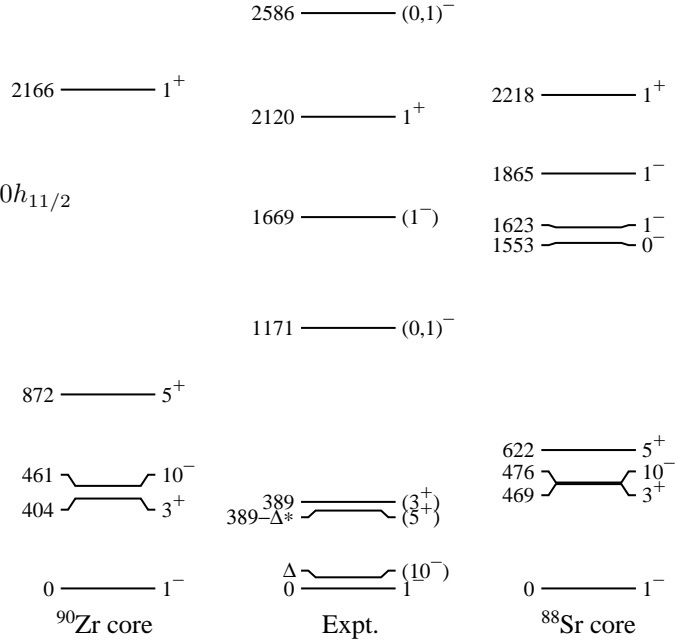


Fig. 1. Comparison of low-energy shell model spectrum for ^{130}In with the data. The shell model spectrum of the left is calculated for the model space assuming a ^{90}Zr core, the one on the right for the model space with a ^{88}Sr core. Details of the calculations are given in the text.

^{130}Cd [19]. It is particularly noteworthy that this includes the excitation energy of the first excited 2^+ state which is calculated at $E_x = 1.325$ MeV in close agreement with the experimental value of 1.346 MeV, hence not confirming the tentative suggestion that this state would reside at $E_x = 0.957$ MeV which had been interpreted as an onset of shell quenching already in ^{130}Cd [20].

As stated above, our calculation of the halfives are based on the valence space on top of the ^{90}Zr as this allows for untruncated calculations and the changes in the computed values of the half-lives are negligible if we adopt the model space with the ^{88}Sr core (and the appropriate interaction).

3 Results

As discussed above, β half-lives depend sensitively on the Q_β value. Unfortunately this important quantity is experimentally not known for most of the relevant $N = 82$ r-process nuclei and hence has to be estimated based on theoretical models or by systematic extrapolations from data for neighboring nuclei. Our Q_β values were calculated from the energies of the isobaric analog states with a systematic correction for the Coulomb displacement energies [23]. In Fig. 2 we compare the shell model Q_β -values with experiment, the Audi-Wapstra systematics [21] and other theoretical calculations. As stated above, our shell model calculation is tuned by proper monopole modifications to reproduce the experimental Q_β value for ^{130}Cd . However, we find also a good agreement to the other Q_β

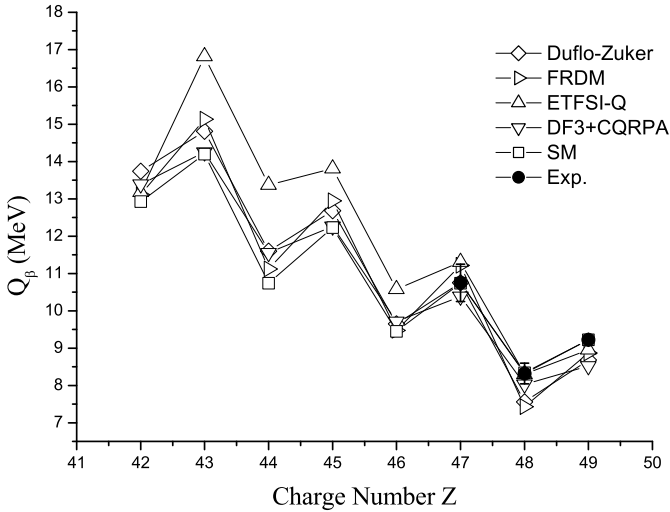


Fig. 2. Comparison of shell model Q_β values for the $N = 82$ isotones to the Audi-Wapstra systematics [21] and to predictions of other models: FRDM [6], ETFSI-Q [22], DF3 [8] and Duflo-Zucker [15].

values as given in the compilation of Audi-Wapstra [21]. Thus as the shell model Q_β values are close to the experimental values and agree with those of most other models within the theoretical uncertainties, we will in the following adopt the shell model Q_β values in our calculation of the half-lives. However, the exception are the predictions of the quenched Extended Thomas-Fermi with Strutinski Integral (ETFSI-Q) model [22] which predicts Q_β -values which are noticeably larger than those of the other models, most noticeably for the most neutron deficient $N = 82$ isotones.

The final ingredients of our half-life calculations are the GT_ strength functions. We have calculated them within our shell model approach using the Lanczos method with 60 iterations for each possible final J -value. The calculated GT_ strength functions for the $N = 82$ nuclei from ^{124}Mo ($Z = 42$) to ^{131}In ($Z = 49$) are shown in Figs. 5-11. For even-even nuclei the GT transitions lead to $J_f^\pi = 1^+$ states in the daughters, while for the odd- A nuclei the final states can have $J_f = J_i - 1, J_i, J_i + 1$, where J_i is the angular momentum of the parent ground state. For the calculation of the half-lives, the choice of the appropriate Gamow-Teller quenching factor is an important issue. It is wellknown that shell model calculations reproduce the GT strength distributions (total strength and fragmentation) very well within complete $0\hbar\omega$ calculations (i.e. model spaces which include a complete major oscillator shell), if the GT operator is quenched by a constant factor. This factor has been determined for sd shell [24,10], where it is 0.77, and the pf shell, where it is 0.74 [25]. Unfortunately the appropriate constant for nuclei in the mass $A = 130$ region has not yet been determined. Thus we adopt a quenching factor of 0.71 adjusted to reproduce the experimental half-life of ^{130}Cd ($t_{1/2} = 162 \pm 7$ ms).

Here one word about first-forbidden transitions is in order. While a study by Möller and collaborators, based

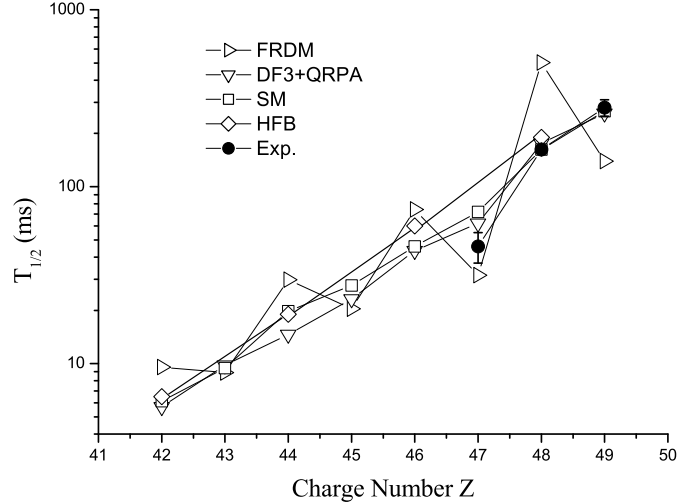


Fig. 3. Comparison of half-lives of the $N = 82$ isotones as calculated in the FRDM [6], HFB [9], and the present shell model approaches with data [4,14].

on the FRDM/QRPA for GT transitions and the statistical gross theory for forbidden theories, indicates sizable contributions of first-forbidden transitions to the half-lives, the only consistent microscopic treatment of GT and first-forbidden transitions for the $N = 82$ half-lives by Borzov, based on the energy density-functional method, implies that forbidden transitions accelerate the half-lives only slightly by about 10% or less. Based on the later result our half-lives calculated purely from GT transitions are meaningful, as a small, but roughly constant contribution of first-forbidden transition can be absorbed into a modification of the quenching factor which would be 0.73 (very close to the standard quenching factor), if first-forbidden transitions yield a 10% contribution.

Our shell model half-life for ^{131}In (260 ms) agrees also with the measured values (280 ± 30 s). However, we overestimate the one for ^{129}Ag slightly (70 ms to be compared with 46^{+5}_-9 s) [26,4]. The present shell-model half-lives are longer for nuclei with $Z \leq 47$ than the ones computed in reference [13] (see table 1). There are two reasons for the change in half-lives. First, for nuclei with $Z = 42-44$ the Q_β -values obtained in the present shell-model calculations are around 1 MeV smaller than the Duflo-Zucker values used in ref. [13] (see fig. 2). Second, for all the nuclei the low lying Gamow-Teller strength is shifted upwards around 0.5 MeV in excitation energy. This shift results in longer half-lives even if the Q_β -value were unmodified as it is the case in ^{129}Ag . This shift is due to the monopole modifications introduced in the interaction used for the present calculations to increase the excitation energy of the 1^+ state in ^{130}In from 1.6 MeV [13] to the experimental value of 2.12 MeV [14].

In Fig. 3 and Table 1 our results are compared with those of other theoretical models and the data. The current half-lives are quite similar to those obtained within the HFB model of [9] and are also in good agreement with the DF3-QRPA approach [27]. The latter is reassuring as the DF3-QRPA model also reproduces the half-lives

Table 1. Comparison of the present shell model half-lives and the ones of reference [13] with experiment [26,4,14]. All half-lives are in ms.

Nucleus	Half-Life (ms)		
	Expt.	Theor.	Theor. (ref [13])
^{131}In	280 ± 30	260	177
^{130}Cd	162 ± 7	162	146
^{129}Ag	46^{+5}_{-9}	70	35.1
^{128}Pd		46	27.3
^{127}Rh		27.65	11.8
^{126}Ru		19.76	9.6
^{125}Tc		9.44	4.3
^{124}Mo		6.13	3.5

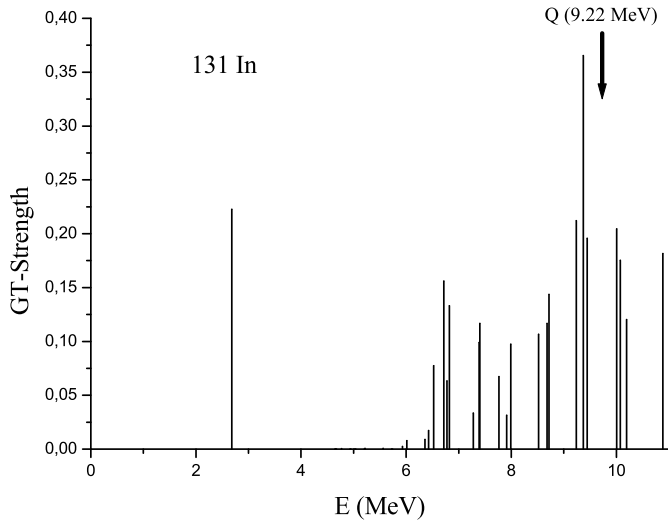


Fig. 4. GT- strength distribution for ^{131}In .

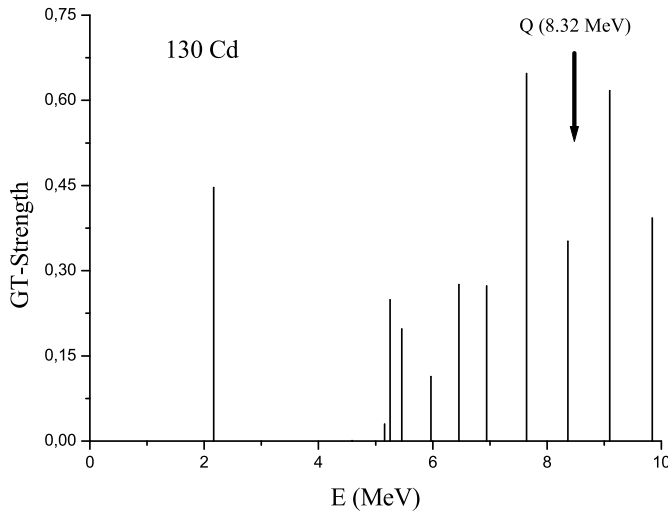


Fig. 5. GT- strength distribution for ^{130}Cd .

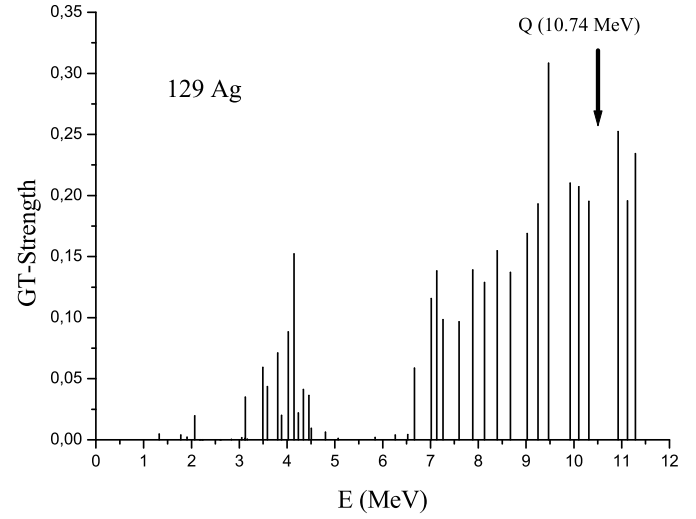


Fig. 6. GT- strength distribution for ^{129}Ag .

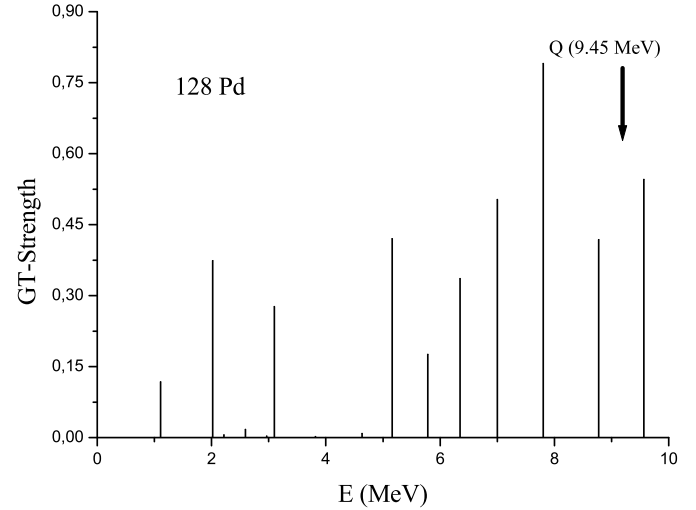


Fig. 7. GT- strength distribution for ^{128}Pd .

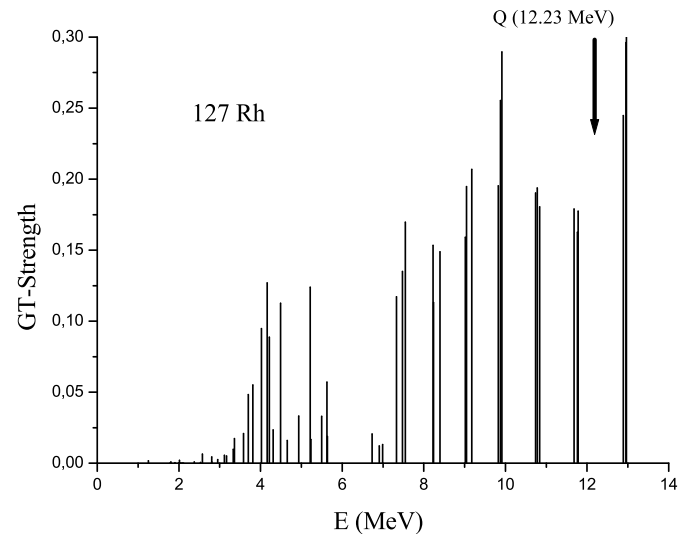
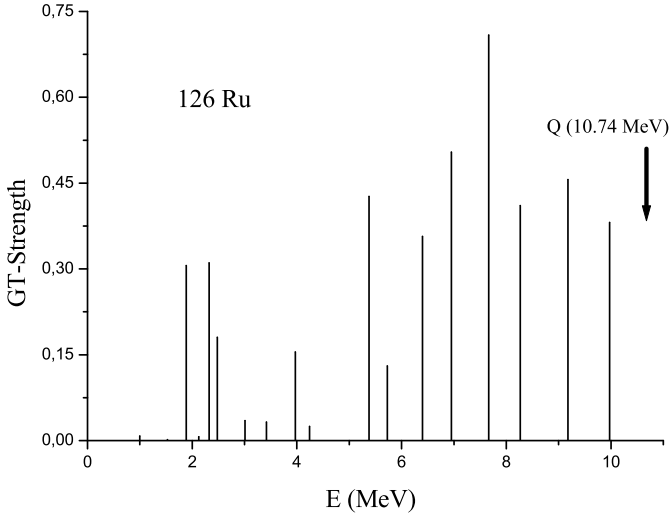
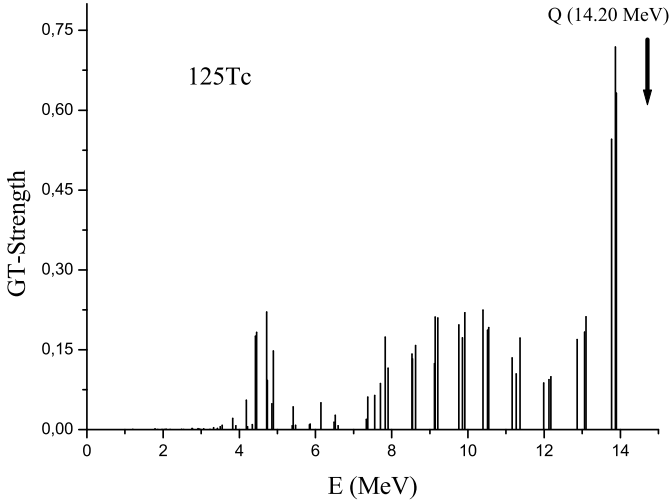
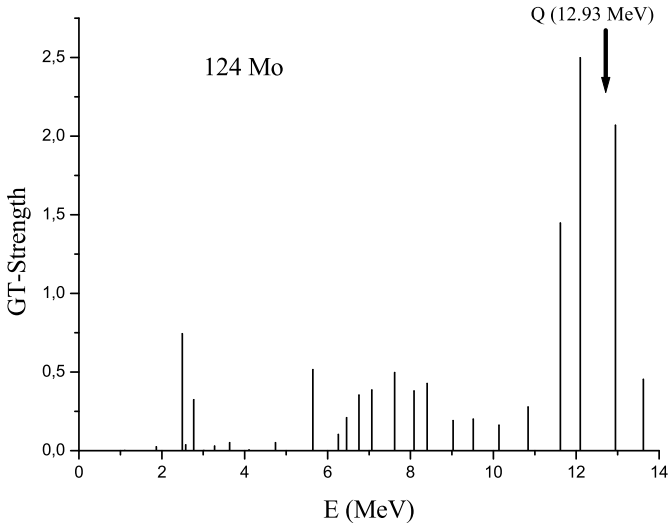
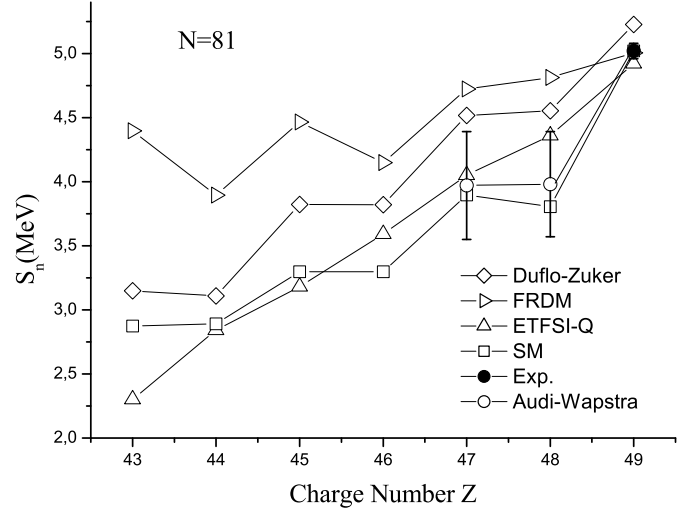


Fig. 8. GT- strength distribution for ^{127}Rh .


Fig. 9. GT₋ strength distribution for ^{126}Ru .

Fig. 10. GT₋ strength distribution for ^{125}Tc .

Fig. 11. GT₋ strength distribution for ^{124}Mo .

Fig. 12. Comparison of the shell model neutron separation energies for the $N = 81$ isotones to the data [21] and predictions of other models: FRDM [6], Duflo-Zucker [15] and ETFSI-Q [22].

of other spherical nuclei in the vicinity of $N = 82$ quite well [28]. Our half-lives show a mild odd-even effect, with the half-lives of the even-even waiting point nuclei slightly enlarged with respect to the neighboring odd- A nuclei. This is caused by a partial cancellation of the odd-even staggering in the Q_β values (Fig. 2) by the larger excitation energies of the lowest GT states in the odd- A daughter nuclei (Figs. 5-11).

As shown in Fig. 2 the various models predict Q_β values within a variation of about 1 MeV, which, due to the strong energy dependence of the phase space, translates into the largest uncertainties of the β half-lives. To estimate this uncertainty we have recalculated the half-lives by replacing the shell model Q_β values by those of the different models and find half-lives which agree with the present ones within a factor of two or better, except for the larger ETFSI-Q Q_β values which result in significantly smaller half-lives for the most proton-deficient nuclei. It is also worth noting that by replacing our shell model Q_β value for ^{129}Ag by the systematic Audi-Wapstra value, we find agreement with the experimental half-life within the uncertainties of the systematic Q_β value.

As the neutron separation energies in the daughter nuclei are quite small, some of the GT₋ strengths resides actually at energies above the neutron emission threshold and β decays to these states are followed by neutron emission. The probability for β -delayed neutron emission depends sensitively on the neutron separation energies S_n which are not known experimentally for most of the nuclei of interest here and have to be estimated theoretically. In Fig. 12 we compare our shell model neutron separation energies for the $N = 81$ daughter nuclei with those of various models. Importantly for ^{131}Sn and ^{130}In the neutron separation energies are known experimentally and our present results agree quite nicely with the data. The neutron separation energies predicted in the FRDM model [6] are larger

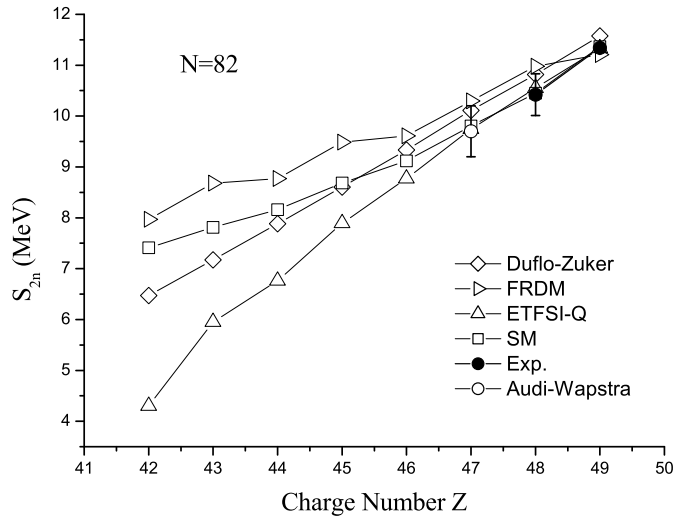


Fig. 13. Comparison of the shell model two-neutron separation energies for the $N = 82$ nuclei to the data [21] and predictions of other models: FRDM [6], Duflo-Zucker [15] and ETFSI-Q [22].

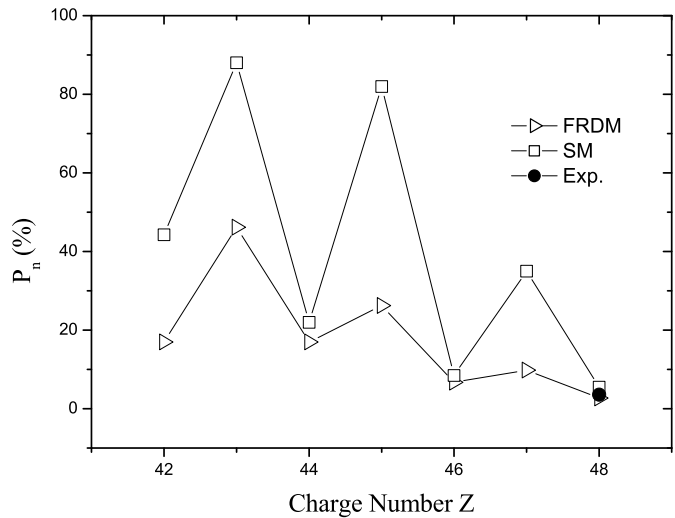


Fig. 14. One neutron emission probabilities.

than all other model predictions and also exceed the experimental values for ^{131}Sn and ^{130}In . Our shell model results predict a quite similar slope of the S_n values as found in the Duflo-Zucker mass model [15] yielding quite sizable neutron separation energies even in the proton-deficient nuclei ^{125}Ru and ^{124}Tc . This is in difference to the ETFSI-Q values [22] which predict a pronounced weakening of the S_n values with increasing neutron excess. A quite similar behavior is found if one compares the 2-neutron separation energies of the $N = 82$ r-process nuclei (Fig. 13). Again, our shell model results agree with the available data (^{131}In and ^{130}Cd) and show a significantly slower decrease of the S_{2n} values than predicted by the ETFSI model, while the FRDM and Duflo-Zucker models yield 2-neutron separation energies which agree reasonably well with the shell model ones.

Using our shell model GT_- strength functions and S_n values we have calculated the probability P_n that the β decay is accompanied by the emission of (at least) one neutron, defined as the relative probability of the β -decay rate above the neutron emission threshold S_n . The results are shown in Fig. 14, indicating that within our shell model study most of the β decays go to states below the neutron threshold for the even-even parent nuclei, yielding probabilities for β -delayed neutron emission of 40% or less. The shell model predicts quite a strong odd-even staggering in the P_n values, indicating P_n values of 80% or larger for ^{127}Rh and ^{125}Tc . The FRDM model [6] also predicts an odd-even dependence in the neutron emission probabilities, however, this effect is somewhat smaller than for the shell model values. For ^{130}Cd , the P_n value is known experimentally [14] and it agrees with the FRDM and shell model predictions.

4 Conclusion

We have recalculated shell model half-lives and neutron emission probabilities for the $N = 82$ waiting point nuclei in the r-process, improving a previous shell model study by enlargement of the model space and by modification of the residual interaction which reproduces recent spectroscopic findings for nuclei in this regime of the nuclear chart. In particular our modified calculation reproduces the unexpectedly high excitation energy of the first 1^+ state in ^{130}In [14]. This, as a good description of the Q_β value, is crucial as the GT transition to this low-lying state dominates the ^{130}Cd half-life. We find good agreement with the experimentally known half-lives for the $Z = 48, 49$ nuclei and overestimate the one of ^{129}Ag slightly.

As in most other models [6,9,7] the shell model half-lives have been computed solely on the assumption of an allowed Gamow-Teller transition. The importance of forbidden transitions for the half-lives of the $N = 82$ waiting point nuclei is somewhat controversial. Using the gross theory for the forbidden transitions, Möller [29] finds non-negligible contributions, while Borzov, adopting the QRPA approach within the Fermi-liquid theory, concludes that forbidden transitions play only a minor role [27]. In view of these differences, shell model calculations of the forbidden β decays of the $N = 82$ r-process waiting point nuclei are desirable.

I. N. Borzov is supported by a grant from the German DFG under contract number 436 RUS 113/907/0-1.

References

1. E. M. Burbidge, G. R. Burbidge, W. A. Fowler, F. Hoyle, *Rev. Mod. Phys.* **29** (1957) 547.
2. A. G. W. Cameron, *Stellar evolution, nuclear astrophysics, and nucleogenesis*, Report CRL-41, Chalk River (1957).
3. J. J. Cowan, F.-K. Thielemann, J. W. Truran, *Phys. Repts.* **208** (1991) 267.

4. B. Pfeiffer, K.-L. Kratz, F.-K. Thielemann, W. B. Walters, Nucl. Phys. A **693** (2001) 282.
5. P. T. Hosmer, *et al.*, Phys. Rev. Lett. **94** (2005) (11) 112501 (pages 4).
6. P. Möller, J. R. Nix, K.-L. Kratz, At. Data. Nucl. Data Tables **66** (1997) 131.
7. I. Borzov, S. Goriely, Phys. Rev. C **62** (2000) 035501, URL <http://www-astro.ulb.ac.be/html/bd.html>.
8. I. Borzov, Nucl. Phys. A **777** (2006) 645.
9. J. Engel, M. Bender, J. Dobaczewski, W. Nazarewicz, R. Surman, Phys. Rev. C **60** (1999) 014302.
10. B. A. Brown, B. H. Wildenthal, Annu. Rev. Nucl. Part. Sci. **38** (1988) 29.
11. E. Caurier, K. Langanke, G. Martínez-Pinedo, F. Nowacki, Nucl. Phys. A **653** (1999) 439.
12. K. Langanke, G. Martínez-Pinedo, Nucl. Phys. A **673** (2000) 481.
13. G. Martínez-Pinedo, K. Langanke, Phys. Rev. Lett. **83** (1999) 4502.
14. I. Dillmann, *et al.*, Phys. Rev. Lett. **91** (2003) 162503.
15. J. Duffo, A. P. Zuker, Phys. Rev. C **52** (1995) R23.
16. E. Caurier, Computer code AN-TOINE, unpublished (1989), URL <http://sbgat194.in2p3.fr/~theory/antoine/main.html>.
17. B. Fogelberg, *et al.*, Phys. Rev. C **70** (2004) (3) 034312 (pages 7).
18. A. Gniady, *et al.*, "to be published" (2007).
19. A. Jungclaus, *et al.*, Nature (2007), "submitted".
20. T. Kautzsch, *et al.* (ISOLDE), Eur. Phys. J. A **9** (2000) 201.
21. G. Audi, A. H. Wapstra, C. Thibault, Nucl. Phys. A **729** (2003) 337.
22. J. M. Pearson, R. C. Nayak, S. Goriely, Phys. Lett. B **387** (1996) 455.
23. M. S. Antony, A. Pape, J. Britz, At. Data Nucl. Data Tables **66** (1997) 1.
24. B. A. Brown, B. H. Wildenthal, At. Data Nucl. Data Tables **33** (1985) 347.
25. G. Martínez-Pinedo, A. Poves, E. Caurier, A. P. Zuker, Phys. Rev. C **53** (1996) R2602.
26. K. L. Kratz, *et al.*, in *Proceedings of the International Conference on Fission and Properties of Neutron-Rich Nuclei*, edited by J. H. Hamilton (World Scientific Press, 1998).
27. I. N. Borzov, Phys. Rev. C **67** (2003) (2) 025802.
28. I. N. Borzov, *et al.*, Phys. Rev. C (2007), to be submitted.
29. P. Möller, B. Pfeiffer, K.-L. Kratz, Phys. Rev. C **67** (2003) 055802.